Activity-dependent inhibitory synapse remodeling through gephyrin phosphorylation

Flores, Carmen E ; Nikonenko, Irina ; Mendez, Pablo ; Fritschy, Jean-Marc ; Tyagarajan, Shiva K ; Muller, Dominique

Abstract: Maintaining a proper balance between excitation and inhibition is essential for the functioning of neuronal networks. However, little is known about the mechanisms through which excitatory activity can affect inhibitory synapse plasticity. Here we used tagged gephyrin, one of the main scaffolding proteins of the postsynaptic density at GABAergic synapses, to monitor the activity-dependent adaptation of perisomatic inhibitory synapses over prolonged periods of time in hippocampal slice cultures. We find that learning-related activity patterns known to induce N-methyl-d-aspartate (NMDA) receptor-dependent long-term potentiation and transient optogenetic activation of single neurons induce within hours a robust increase in the formation and size of gephyrin-tagged clusters at inhibitory synapses identified by correlated confocal electron microscopy. This inhibitory morphological plasticity was associated with an increase in spontaneous inhibitory activity but did not require activation of GABAA receptors. Importantly, this activity-dependent inhibitory plasticity was prevented by pharmacological blockade of Ca(2+)/calmodulin-dependent protein kinase II (CaMKII), it was associated with an increased phosphorylation of gephyrin on a site targeted by CaMKII, and could be prevented or mimicked by gephyrin phospho-mutants for this site. These results reveal a homeostatic mechanism through which activity regulates the dynamics and function of perisomatic inhibitory synapses, and they identify a CaMKII-dependent phosphorylation site on gephyrin as critically important for this process.

DOI: https://doi.org/10.1073/pnas.1411170112

Biological sciences, neuroscience

Activity-dependent inhibitory synapse formation through gephyrin phosphorylation

Carmen E. Flores[1], Irina Nikonenko[1], Pablo Mendez[1], Jean-Marc Fritschy[2], Shiva K. Tyagarajan[2]* & Dominique Muller[1]*

[1]Département des Neurosciences Fondamentales, Université de Genève, Faculté de Médecine, Centre Médical Universitaire, 1 Michel Servet, 1211 Genève 4

[2]Institute of Pharmacology and Toxicology, University of Zürich, Switzerland.

*equal contribution

Correspondence: Dominique Muller, Département des Neurosciences Fondamentales, Centre Médical Universitaire, 1211 Geneva 4, Switzerland

Short title: inhibitory synapse formation and gephyrin

Keywords: Gabaergic synapses, inhibition, homeostatic plasticity, rat, hippocampus

AUTHOR CONTRIBUTIONS: C.E.F., I.N., P.M., S.T. and D.M. designed the experiments. C.E.F. I.N., P.M., and S.T. performed experiments, S.T. and J-M.F. generated tools and provided antibodies, C.E.F., S.T. and D.M. wrote the paper.

Abstract

Maintaining a proper balance between excitation and inhibition is essential for the functioning of neuronal networks. However little is known about the mechanisms through which excitatory activity can affect inhibitory synapse plasticity. Here we used tagged gephyrin, one of the main scaffolding proteins of the postsynaptic density at GABAergic synapses, to monitor the activity-dependent adaptation of perisomatic inhibitory synapses over prolonged periods of time in hippocampal slice cultures. We find that learning-related activity patterns known to induce NMDAR-dependent long-term potentiation (LTP) as well as transient optogenetic activation of single neurons induce within hours a robust increase in the formation and size of gephyrin-tagged clusters at inhibitory synapses identified by correlated confocal electron microscopy. This inhibitory morphological plasticity was associated with an increase in spontaneous inhibitory activity, but did not require activation of GABAA receptors. Importantly, this activity-dependent inhibitory plasticity was prevented by pharmacological blockade of CaMKII, it was associated with an increased phosphorylation of gephyrin on a site targeted by CaMKII and could be prevented or mimicked by gephyrin phospho-mutants for this site. These results reveal a new homeostatic mechanism through which activity regulates the dynamics and function of perisomatic inhibitory synapses and they identify a CaMKII dependent phosphorylation site on gephyrin as critically important for this process.

Significance statement

Learning mechanisms rely on plasticity properties of excitatory synapses and an activity-dependent rewiring of excitatory networks. Inhibitory synapses also display plasticity properties, but it remains unknown whether and how excitatory activity and plasticity can affect the organization of inhibitory networks. Here we show that synaptic and neuronal activity directly regulates the number and function of perisomatic inhibitory synapses through a mechanism that involves the phosphorylation of gephyrin by the enzyme calcium/calmodulin-dependent protein kinase II. The results identify a new homeostatic mechanisms through which cell activity can continuously adjust its excitation/inhibition balance.

\body

Introduction

Several activity-dependent plasticity and homeostatic mechanisms (1, 2) contribute to regulate synaptic strength at excitatory synapses. Similar mechanisms are also expected to finely tune the level of inhibition in response to activity in individual neurons, but the mechanisms remain poorly understood. Several forms of plasticity of GABAergic transmission have been reported based on either pre- or postsynaptic mechanisms (3, 4). Similarly to excitatory receptors, $GABA_A$ receptors ($GABA_ARs$), which mediate the fast component of inhibitory transmission, display complex trafficking mechanisms that affect the surface localization and diffusion of the receptors (5). The distribution and clustering of $GABA_ARs$ at synapses is tightly regulated through interactions with the scaffolding protein gephyrin, one of the main structural constituent of inhibitory postsynaptic densities. Gephyrin forms multimeric complexes that allow the anchoring of $GABA_ARs$ (6) through molecular mechanisms that include phosphorylation and interactions with the guanine-nucleotide-exchange factor collybistin (7-12). In addition to changes in inhibitory strength, more recent *in vivo* experiments revealed that inhibitory synapses are also dynamic structures that can be formed and eliminated in response to sensory experience (13-15). It remains however unknown whether excitatory activity can directly control the number and properties of inhibitory synapses. We investigated here this issue using repetitive confocal imaging of tagged gephyrin to monitor the dynamic behavior of inhibitory synapses over periods of days. Our results show that induction of synaptic plasticity and neuronal activity induces the formation of new perisomatic inhibitory synapses through postsynaptic mechanisms involving the phosphorylation of gephyrin at a CaMKII dependent site.

Results

Turnover and correlated confocal electron microscopy of gephyrin clusters

We transfected rat hippocampal slice cultures with fluorescently-tagged gephyrin and 8 days after transfection, we monitored the behavior of identified gephyrin clusters over several days (Fig.1A-B). These analyses revealed that gephyrin clusters are dynamic structures that are continuously formed and eliminated over time. The basal level of turnover observed in 19 days in vitro (DIV19) slices averaged 13.6$\pm$3.5% for newly-formed clusters and 18.1±3.8% for eliminated clusters (Fig.

1C, suppl. Table 1) per 24h. This turnover occurred without significant changes in either cluster density or size over time (Fig.1D-E). As illustrated in figure 1A, gephyrin clusters showed large variations in size. The vast majority of clusters (>90%) were of small size (<0.5 μm^2), corresponding to the size of gephyrin clusters revealed by immunofluorescence (suppl. Fig.1) or by quantitative nanoscopic imaging (16).

To verify that fluorescent gephyrin clusters corresponded to inhibitory synapses, we used a correlated confocal electron microscopy (EM) approach to reconstruct dendritic segments of transfected pyramidal neurons (Fig. 1F). Inhibitory synapses were identified by the presence of a symmetric apposition between a postsynaptic density and a presynaptic terminal, filled with pleomorphic synaptic vesicles forming an active zone (17). A high level of correlation was observed between the presence of gephyrin clusters and the identification of inhibitory synapses. All gephyrin clusters had at least one corresponding inhibitory synapse identified at the EM level. Large clusters usually correlated with the presence of several inhibitory synapses. A few inhibitory synapses observed at the EM level had no detectable corresponding fluorescent signal (87.5% correlation between EM synapses and confocal clusters).

Activity-dependent formation of new gephyrin clusters

We then investigated whether synaptic activation of transfected neurons could affect the dynamics of gephyrin clusters. We first induced transient theta activity in organotypic hippocampal slices by applying the cholinergic agonist carbachol (Cch, 10 µM) for a short period of time (45 min). Cch treatment produced a significant increase in the proportion of new gephyrin clusters detected over the next 24h (Cch, 106.7±21.4%, n=4 cells; Ctrl, 13.6±3.5%, n=4 cells; Fig. 2A,C, suppl. Table 1) with no significant changes in the proportion of lost clusters (Fig. 2D, suppl. Table 1). These turnover changes resulted in a significant increase in normalized density (1.8±0.2 per 24h) and were associated with an increase in size of gephyrin clusters (Fig. 2E, suppl. Table 1). Immunolabeling at 72h for the presynaptic inhibitory marker GAD67 (glutamic acid decarboxylase) revealed a close apposition between all newly-formed gephyrin clusters and GAD67 immunostaining suggesting that they represented new inhibitory synapses.

We then applied a short theta burst stimulation (TBS) protocol that induces LTP in slice cultures (18). Similar to the carbachol treatment, TBS also produced a marked increase in the formation of

new gephyrin clusters 24h after stimulation (TBS, 63.0±12.0%, n=7 cells; Fig. 2B,C, suppl. Table 1), but no changes in the proportion of lost clusters (Fig. 2D). Additionally, pre-existing gephyrin clusters showed a robust increase in size (Fig. 2E, suppl. Table 1). To verify that these new clusters represented inhibitory synapses, we performed 3D EM reconstruction of mCherry-gephyrin transfected neurons following TBS. As illustrated in figure 3G, all new gephyrin clusters observed 24h after TBS could be related to symmetric synapses or clusters of inhibitory contacts identified on 3D reconstruction, supporting the notion that they represented newly formed synapses. In order to determine the specificity of these changes, we also applied TBS, but in the presence of the N-methyl-D-aspartate (NMDA) receptor antagonist (D-AP5; 50 µM). As shown in figure 3C-E, D-AP5 prevented the increase in number (TBS, 15.0±4.9%, n=6 cells) and size (0.31±0.05 μm^2, 24h, suppl. Table 1) of gephyrin clusters.

Mechanisms underlying activity-dependent formation of new gephyrin clusters

To investigate the mechanisms underlying the activity-dependent formation of gephyrin clusters, we tested the effects of the $GABA_AR$ antagonist gabazine (GBZ), which enhances excitatory activity while blocking inhibition. Application of GBZ (15 µM) to slice cultures for 45-60 min produced a robust increase in the formation of new gephyrin clusters over the next 24h (GBZ, 89.4±14.5%, n=7 cell, Fig. 3A-B, suppl. Table 1) as well as an increase in their size (GBZ, Fig. 3C, suppl. Table 1). To investigate the functional implications of this morphological inhibitory plasticity, we performed whole cell recordings in GBZ-treated, non-transfected neurons. Analysis of spontaneous activity showed a significant increase in frequency (Ctrl, 1.06±0.12 Hz, n=11 cells; GBZ, 1.60±0.19 Hz, n=11 cells; $p < 0.05$; Fig. 3D-E) and amplitude (Ctrl, 18.8±1.9 pA, n=10 cells; GBZ, 27.8±2.9 pA, n=11 cells; $p < 0.05$; Fig. 3D-E) of miniature inhibitory postsynaptic currents (mIPSC), indicating that these new synapses were functional. Thus postsynaptic activation of inhibitory synapses is not required for the induction of this inhibitory plasticity.

We then targeted individual pyramidal neurons and tested whether cellular activity, independently of synaptic inputs, could affect the dynamics of gephyrin-containing inhibitory synapses. Hippocampal cultures were co-transfected with mCherry-gephyrin and Channelrodhopsin-2 Venus (ChR2 Venus; Fig.4A) and stimulated using a 470 nm light pulse protocol (trains of 5 pulses at 10Hz, repeated at 1Hz for 5 min). This light stimulation paradigm reproducibly evoked action

potentials in individual neurons (Fig. 4B; see Methods for details). Analysis of transfected neurons before and 24h after light stimulation revealed that neurons exposed to 470 nm light pulses (blue), but not neurons exposed to 625 nm light pulses (red) showed very robust structural changes. The proportion of newly formed gephyrin clusters (red light: 16.9±4.4%, n=4 cells; blue light: 63.1±24.4%, n=5 cells; Fig. 4C-F, suppl. Table 1) as well as their size (Fig. 4G, suppl. Table 1) strongly increased 24h after stimulation. Similar results were also obtained when light stimulation was applied in the presence of glutamate receptor antagonists. These experiments thus indicated that cell spiking was sufficient for promoting inhibitory synapse formation.

Role of CaMKII and gephyrin phosphorylation in gephyrin cluster plasticity

To investigate the molecular mechanisms underlying this activity-dependent inhibitory plasticity, we first examined a possible implication of multifunctional Ca2+/calmodulin-dependent protein kinase II (CaMKII), which was recently shown to accumulate at inhibitory synapses following short NMDA and glutamate stimulation (19). Treatment of slice cultures with the CaMKII inhibitor KN-93 (10 µM) during TBS fully prevented the activity-dependent increase in gephyrin cluster formation and size (Fig. 5A-C). We then looked for a possible target of CaMKII. As gephyrin phosphorylation is implicated in $GABA_A$Rs clustering (8), we analyzed CaMKII phosphorylation sites on gephyrin. *In silico* analysis of rat gephyrin sequences (NP_074056.2) identified two residues, S303 and S305, that had a strong consensus for CaMKII phosphorylation. An *in vitro* kinase assay with bacterially expressed and purified gephyrin and active forms of CaMKII and PKA confirmed that S305 site is a target of CaMKII, whereas S303 site is phosphorylated by PKA (Suppl. Fig. 2). Furthermore induction of inhibitory synapse formation by GBZ (15 µM) resulted in an enhanced phosphorylation of S305 site 8 hours after treatment (Fig. 5C). We then generated S303D/S305D (phospho-mimetic) and S303A/S305A (phospho-deficient) eGFP-gephyrin mutants to test the functional role of gephyrin phosphorylation in inhibitory synapse plasticity. Analysis of fluorescent gephyrin cluster turnover 8 days after transfection showed that the S303A/S305A phospho-resistant mutant did not affect basal gephyrin cluster dynamics as compared to wild type gephyrin expression (Fig. 5E: Ctrl and SSA grey columns, Suppl. Table 1). In contrast, expression of the S303D/S305D phospho-mimetic mutant resulted in a significant increase in the basal rate of cluster formation per 24h (Fig. 5D,E: Ctrl and SSD grey columns, Suppl. Table 1) as well as changes in cluster size (Fig. 5F: grey

columns, Suppl. Table 1). Next, we tested how the phospho-mutants affected activity-dependent gephyrin cluster formation following TBS. Expression of the phospho-resistant SSA mutant fully prevented activity-dependent formation of new gephyrin cluster (Fig. 5E: SSA and SSA+TBS columns, Suppl. Table 1), indicating that gephyrin phosphorylation is necessary for activity-dependent inhibitory synapse formation. Conversely, expression of the phospho-mimetic SSD mutant increased gephyrin cluster formation under basal conditions (Fig. 5D), an effect that occluded further increases produced by TBS (Fig. 5E: SSD and SSD+TBS columns, Suppl. Table 1). These results thus indicate that phosphorylation of gephyrin on the S303 and S305 sites is both sufficient and necessary to promote inhibitory synapse formation in response to neuronal activity. Note that expression of the phospho-resistant S303A/S305A mutant also prevented all changes in size of gephyrin clusters by stimulation (Fig. 5F: SSA and SSA+TBS columns, Suppl. Table 1). Interestingly, the differential regulation of cluster size by activity remained preserved with expression of the phospho-mimetic mutant, independently of the effects on dynamics (Fig. 5F: SSD and SSD+TBS columns, Suppl. Table 1). This result suggests that the regulation of gephyrin cluster size by activity requires additional partners or mechanisms.

Discussion

Work over the last decade has provided strong evidence indicating that behavioral experience and learning related activity patterns can promote rearrangements of excitatory synaptic networks (20). The present study now demonstrates that the same activity patterns and neuronal firing also promote re-arrangements of perisomatic inhibitory synapses in the hippocampus, providing a new homeostatic mechanism to control pyramidal neurons excitabillity. Furthermore our results show that this structural inhibitory plasticity is independent of the activation of GABAergic inhibitory synapses, but mediated by postsynaptic mechanisms involving a CaMKII-dependent phosphorylation of gephyrin, since gephyrin phospho-mutants were able to reproduce or prevent activity-dependent inhibitory synapse plasticity.

Although synaptic plasticity mechanisms have been mainly studied at excitatory synapses, accumulating evidence indicates that inhibitory synapses are also characterized by forms of plasticity. Changes in strength of GABAergic transmission have now been reported at many inhibitory synapses (3, 4)(21) and shown to involve different molecular events (22, 23). The notion

that inhibitory synapses could also be structurally plastic and undergo continuous re-arrangements is however much less understood. Recent *in vivo* studies have showed that sensory activity or ocular dominance plasticity are associated with important changes in the kinetics and clustering of dendritic inhibitory synapses (14, 15, 24). Here we focused on perisomatic inhibition, which is mainly mediated by parvalbumin interneurons and represents the main inhibitory input to hippocampal CA1 pyramidal neurons (25). These GABAergic synapses play an essential role in the control of network activity and gamma oscillations (26, 27). Using tagged-gephyrin as a marker of inhibitory synapses, our study shows that patterns of high frequency activity and neuronal firing promote the formation over 24h of new gephyrin clusters. Several findings suggest that these new gephyrin clusters are new inhibitory synapses. Their size correspond to that of puncta revealed by endogenous gephyrin immunostaining and values obtained by nanoscopic analysis of gephyrin clusters (16). The new gephyrin clusters detected after stimulation display co-localization with GAD67 immunostaining and correlate with the presence of inhibitory symmetric synapses revealed by 3D EM reconstruction. The few inhibitory synapses that were not detected at the confocal level, as previously observed with similar approaches (14, 15) cannot account for the changes reported here. Finally, the whole cell recordings also indicate an increased number and efficacy of inhibitory synapses. Altogether, these results support the conclusion that synaptic and neuronal activity promoted the formation of new perisomatic inhibitory contacts.

Our experiments further identify two phosphorylation sites on gephyrin that appear to be both necessary and sufficient for the formation of new inhibitory synapse by activity. The critical involvement of gephyrin in these mechanisms is consistent with several recent data highlighting its implication in the clustering of $GABA_A$Rs. Phosphorylation of gephyrin on Ser270 by glycogen synthase kinase 3beta (GSK3beta) or on Ser268 by ERK have been shown to modulate the density and size of gephyrin clusters (8, 28). Also gephyrin can interact with various partners, including neuroligin 2, collibystin or even Cdc42 to regulate cluster formation and $GABA_A$R aggregation (7, 9). These results are thus consistent with the idea that gephyrin acts as a molecular hub regulating the formation and extension of the inhibitory postsynaptic density (12). Our data now indicate that gephyrin phosphorylation on Ser303 and Ser305 sites could play a critical role in the activity-dependent regulation of these clustering mechanisms. Our results further suggest that CaMKII is likely to be one of the important kinases implicated in this effect.

Pharmacological blockade of CaMKII prevented gephyrin cluster dynamics and S305 phosphorylation is enhanced following neuronal activation. The situation regarding Ser303 is less clear, but suggests that PKA could also be implicated. Thus the enzymes that play a key role in mechanisms of excitatory synapse plasticity (29) also mediate a compensatory increase of inhibitory synapses.

Altogether our data identify a new mechanism through which neuronal activity can exert an homeostatic control of the number and function of perisomatic inhibitory synapses. This phenomenon may be critically important to individually optimize the level of inhibition on pyramidal neurons and thus set the proper balance required for the synchronization of oscillations mediated by parvalbumin interneurons during learning (26, 30, 31).

Methods

Organotypic Hippocampal Cultures. Organotypic hippocampal slice cultures (400 µm of thickness) were prepared from 6- to 7-days old rat pups (32) and transfected at DIV11 using a biolistic approach (DNA-coated gold microcarriers; 1.6 µm with a Helios Gene Gun, Bio-Rad Laboratories) according to the instructions of the manufacturer. A few cells were usually transfected per slice and only one cell per slice was analyzed using repetitive confocal microscopy 7-8 days after transfection in order to obtain consistent tagged gephyrin expression.

Plasmids and gephyrin phosphorylation mutants. To visualize inhibitory synapses, we used eGFP-gephyrin (28) as well as mCherry-gephyrin (8). The double gephyrin mutants of the S303 and S305 residues were identified as putative CaMKII phosphorylation sites by in silico analyses (NP_074056.2). The double mutant eGFP-S303/S305A and eGFP-S303D/S305D gephyrin were generated using a site directed mutagenesis protocol (Life Technologies, USA). The mutation sequences were confirmed and checked for protein expression prior to neuron transfection.

Imaging. Laser scanning confocal microscopy was performed using an Olympus Fluoview 300 system. Proximal dendrites of CA1 hippocampal pyramidal neurons expressing tagged gephyrin were imaged 8 days after transfection at DIV19 for several days as described (18). For quantitative analyses, maximum intensity projections were used and images of proximal dendrites were thresholded from background with an scaling factor of 3 (segmentation plugin, NIH image J). Gephyrin clusters were identified (ROI) using a multi-particle analysis by size discrimination (>0.02

μm^2, NIH image J) and ROI area values were obtained from the z-stack of raw images using Multi Measure tool. For presentation purposes, some images were processed with NIH Image J and OsiriX software for volume rendering.

Electron Microscopy. For correlative confocal and electron microscopy (EM), hippocampal slice cultures with CA1 pyramidal neurons co-transfected with eGFP and mCherry-gephyrin were first imaged in a confocal microscope, fixed immediately after and processed for eGFP immunoperoxidase EM labeling as described (33). After embedding in EPON resin (Fluka), the slices were trimmed around the imaged neurons and serial ultrathin (60 nm) sections were cut. Images of the labeled primary apical dendrites of interest were taken at magnification x9700 (Tecnai G212, FEI Company; Eindhoven, Netherlands). After alignment of digital serial electron micrographs using Photoshop software (Adobe, San Jose, CA, USA), complete 3D reconstruction of the dendritic segment of interest was carried out using Neurolucida software (version 6.02; MicroBrightField, Inc.). Inhibitory synaptic contacts were defined by the presence of the close apposition of a presynaptic bouton, filled with pleomorphic synaptic vesicles forming an active zone with docked vesicles, with the labeled apical dendrite.

Optogenetic stimulation. Slice cultures were transfected with Channelrhodopsin2-venus (ChR2-venus) and mCherry-gephyrin using the gene gun approach. 8 days after transfection they were transferred to a recording chamber and optogenetic stimulation was carried out using laser-emitting diodes (LEDs, 488nm and 625nm). A 625 nm red light spot of approximately 100 µm in diameter was used to position the focus of the light over the cell of interest. Optogenetic stimulation was performed using light pulses of 20ms duration with a nominal power at the exit of 0.790 and 0.653 mW for blue and red light respectively. The stimulation protocol consisted in 5 pulses at 10Hz repeated every second during 5 minutes (1500 pulses).

Electrophysiology. Stimulation of slice cultures was carried out in an interface chamber as described (18). They were continuously perfused (2–2.5 ml/min) with a solution containing (in mM): NaCl 124, KCl 1.6, CaCl2 2.5, MgCl2 1.5, NaHCO3 24, KH2PO4 1.2, glucose 10, ascorbic acid 2; saturated with 95% O2 and 5% CO2 (pH 7.4; temperature 31°C). Tetrodotoxin (TTX 1 µM) and SR95531 (10 µM) were added to the perfusion solution for spontaneous inhibitory miniature recordings (mIPSC). Whole-cell recordings were carried out using patch pipettes filled with a solution containing (in mM): 70 Kgluconate, 70 KCl, 2 NaCl, 2 $MgCl_2$, 10 HEPES, 1 EGTA, 2

MgATP, and 0.3 Na_2GTP, pH 7.3 corrected with KOH (290 mOsm). Under these recording conditions, activation of $GABA_A$ receptors resulted in inward currents at a holding potential (V_h) of -70 mV (E_{GABA} was approximately -15 mV). Recordings were obtained using an Axopatch 200B (Molecular Devices), filtered at 2 kHz, and digitized at 5–10 kHz and stored on hard disk. Data acquisition and analysis were performed using pClamp 9. Custom written software (Detector, courtesy J. R. Huguenard, Stanford University) was used for analyzing miniature IPSCs events.

Immunohistochemistry. Slices were fixed using 2% cold paraformaldehyde in 0.1 M phosphate buffer for 1 hour, rinsed with phosphate buffer saline (PBS), pH 7.4 for 45 min and then simultaneously blocked and permeabilized for 1h at room temperature in PBS containing 0.5–1% Triton X-100, 5-10% normal goat serum (NGS), and 1-2 % bovine serum albumin (BSA), pH 7.4. Slices were then incubated overnight at 4°C in a tilting platform with either mouse monoclonal anti-GAD67 (1:5000) (MAB 5406, clone 1G10.2. Millipore) or anti-gephyrin (1:500) (147021, clone mAb7; SYSY) antibodies dissolved in PBS containing 0.5% Triton X-100, 5% NGS, and 0.5% BSA, pH 7.4. After primary antibody incubation, slices were washed and incubated with Alexa Fluor 488 or 647 donkey anti-mouse (1:500) (A21202, A11008, Invitrogen) secondary antibodies. The slices were mounted on slides in a 0.2% n-propyl gallate-based antifading solution. Sections were acquired with a confocal laser scanning microscope (LSM 510 Meta; Carl Zeiss) with 40x 0.8W (3.6 mm) objective lens. Images were background subtracted and thresholded using NIH Image J to include signals at least 2- to 3-fold greater than the background signal.

Mouse brain extract and in-vitro kinase assay. 3 months old mice whole brain extract was prepared through homogenization using EBC buffer in the presence of protease inhibitor cocktail (Roche) and phosphatase inhibitor 2 and 3 (Sigma). The total cell lysate was collected after ultracentrifugation of the samples at 50,000 rpm for 60min at 4^{o}C. 12ml of the sample was loaded on 8% SDS PAGE gel and probed using either phospho-gephyrin S303, phospho-gephyrin S305 and detected using HRP conjugated donkey secondary antibody (Jackson labs).

In vitro kinase assay was performed using purified full-length STREP-gephyrin expressed in bacteria (8). The purified gephyrin was phosphorylated in PKA kinase buffer (50 mm MOPS pH 6.5, 100 µm ATP, 10 mm $MgCl_2$, 10mm DTT, 1 mg/mL BSA, and H_2O to a final volume of 50 µl) or CaMKII kinase buffer (1x PK buffer, 1x $CaCl_2$, 1x CaM and water to 50 ml) and purified activated PKA 0.5 µl (Calbiochem) or 1ml CaMKII (NEB) was added and samples incubated at 30°C for 30

min. The samples were washed in EBC buffer to remove all unbound kinase and proteins prior to addition of 2× SDS loading buffer and boiling at 90 °C for 3 min. WB to detect gephyrin phosphorylation was performed using either anti-phospho-gephyrin Ser-303 (1 µg/ml, custom made by Genscript) or Ser-305 (1mg/mL, custom made by Genscript) and commassie stain to detect total gephyrin.

Western blots. Slice cultures (16-20 DIV) were rapidly stored at −80°C until homogenization. Tissue was lysed in EBC buffer (50 mM Tris pH 7.4-8, 120 mM NaCl, 0.5% Nonidet P-40) containing complete mini-protease inhibitor (Roche Diagnostics) and phosphatase inhibitors (Sigma-Aldrich). Homogenates were sonicated at 4°C, centrifuged for 20 min at 14,000 × *g* at 4°C, and the supernatant was collected. Protein was quantified using BCATM Protein Assay Kit (Pierce) and 20 µl of samples (containing 40 µg of protein) were resolved on Bis-Tris Protein Gels 4-12% (NuPAGE). In order to detect gephyrin phosphorylation, membranes were blocked for 1 hour at room temperature with 5% nonfat dry milk in TBS and then probed using either mouse monoclonal gephyrin antibody (1 to 1000) (3B11, SYSY) or phospho-gephyrin S305 (1 mg/mL, custom made by Genscript), or rabbit polyclonal GAPDH antibody (1 to 50000) (Sigma) antibodies and detected using HRP conjugated donkey secondary antibody (Jackson labs). Protein were resolved by chemiluminescence ECL (GE Healthcare).

Statistical analyses

Graphs and statistical analyses were carried out with Prism. Data and statistics are given for each experimental condition in Suppl. Table 1. Statistical analyses were performed using either one-way ANOVA with Bonferroni post-tests or Mann-Whitney U-test. Data are represented as mean ± standard error of the mean. Data significance is indicated as follows: *:$p<0.05$, **:$p<0.01$, ***:$p<0.001$.

Acknowledgements: We thank Yann Bernardinelli and Lorena Jourdain for their support and excellent technical help. This work was supported by SNF grant Sinergia and grant 310030B-144080 to D.M.

References

1. Malinow R, Malenka RC (2002) AMPA receptor trafficking and synaptic plasticity. *Annu Rev Neurosci* 25:103–126.
2. Turrigiano GG, Nelson SB (2004) Homeostatic plasticity in the developing nervous system. *Nat Rev Neurosci* 5:97–107.
3. Nugent FS, Penick EC, Kauer JA (2007) Opioids block long-term potentiation of inhibitory synapses. *Nature* 446:1086–1090.
4. Petrini EM, Ravasenga T, Hausrat TJ, Iurilli G, Olcese U, Racine V, Sibarita JB, Jacob TC, Moss SJ, Benfenati F *et al.* (2014) Synaptic recruitment of gephyrin regulates surface GABAA receptor dynamics for the expression of inhibitory LTP. *Nat Commun* 5:3921.
5. Jacob TC, Moss SJ, Jurd R (2008) GABA(A) receptor trafficking and its role in the dynamic modulation of neuronal inhibition. *Nat Rev Neurosci* 9:331–343.
6. Fritschy JM, Panzanelli P, Tyagarajan SK (2012) Molecular and functional heterogeneity of GABAergic synapses. *Cell Mol Life Sci* 69:2485–2499.
7. Poulopoulos A, Aramuni G, Meyer G, Soykan T, Hoon M, Papadopoulos T, Zhang M, Paarmann I, Fuchs C, Harvey K *et al.* (2009) Neuroligin 2 drives postsynaptic assembly at perisomatic inhibitory synapses through gephyrin and collybistin. *Neuron* 63:628–642.
8. Tyagarajan SK, Ghosh H, Yevenes GE, Nikonenko I, Ebeling C, Schwerdel C, Sidler C, Zeilhofer HU, Gerrits B, Muller D *et al.* (2011) Regulation of GABAergic synapse formation and plasticity by GSK3beta-dependent phosphorylation of gephyrin. *Proc Natl Acad Sci U S A* 108:379–384.
9. Tyagarajan SK, Ghosh H, Harvey K, Fritschy JM (2011) Collybistin splice variants differentially interact with gephyrin and Cdc42 to regulate gephyrin clustering at GABAergic synapses. *J Cell Sci* 124:2786–2796.
10. Mayer S, Kumar R, Jaiswal M, Soykan T, Ahmadian MR, Brose N, Betz H, Rhee JS, Papadopoulos T (2013) Collybistin activation by GTP-TC10 enhances postsynaptic gephyrin clustering and hippocampal GABAergic neurotransmission. *Proc Natl Acad Sci U S A* 110:20795–20800.
11. Vlachos A, Reddy-Alla S, Papadopoulos T, Deller T, Betz H (2013) Homeostatic regulation of gephyrin scaffolds and synaptic strength at mature hippocampal GABAergic postsynapses. *Cereb Cortex* 23:2700–2711.
12. Tyagarajan SK, Fritschy JM (2014) Gephyrin: a master regulator of neuronal function? *Nat Rev Neurosci* 15:141–156.
13. Dobie FA, Craig AM (2011) Inhibitory synapse dynamics: coordinated presynaptic and postsynaptic mobility and the major contribution of recycled vesicles to new synapse formation. *J Neurosci* 31:10481–10493.

14. Chen JL, Villa KL, Cha JW, So PT, Kubota Y, Nedivi E (2012) Clustered dynamics of inhibitory synapses and dendritic spines in the adult neocortex. *Neuron* 74:361–373.
15. van Versendaal D, Rajendran R, Saiepour MH, Klooster J, Smit-Rigter L, Sommeijer JP, De Zeeuw CI, Hofer SB, Heimel JA, Levelt CN (2012) Elimination of inhibitory synapses is a major component of adult ocular dominance plasticity. *Neuron* 74:374–383.
16. Specht CG, Izeddin I, Rodriguez PC, El Beheiry M, Rostaing P, Darzacq X, Dahan M, Triller A (2013) Quantitative nanoscopy of inhibitory synapses: counting gephyrin molecules and receptor binding sites. *Neuron* 79:308–321.
17. Lushnikova I, Skibo G, Muller D, Nikonenko I (2011) Excitatory synaptic activity is associated with a rapid structural plasticity of inhibitory synapses on hippocampal CA1 pyramidal cells. *Neuropharmacology* 60:757–764.
18. De Roo M, Klauser P, Muller D (2008) LTP promotes a selective long-term stabilization and clustering of dendritic spines. *PLoS Biol* 6:e219.
19. Marsden KC, Shemesh A, Bayer KU, Carroll RC (2010) Selective translocation of Ca2+/calmodulin protein kinase IIalpha (CaMKIIalpha) to inhibitory synapses. *Proc Natl Acad Sci U S A* 107:20559–20564.
20. Caroni P, Donato F, Muller D (2012) Structural plasticity upon learning: regulation and functions. *Nat Rev Neurosci* 13:478–490.
21. Kullmann DM, Moreau AW, Bakiri Y, Nicholson E (2012) Plasticity of inhibition. *Neuron* 75:951–962.
22. Kano M, Ohno-Shosaku T, Hashimotodani Y, Uchigashima M, Watanabe M (2009) Endocannabinoid-mediated control of synaptic transmission. *Physiol Rev* 89:309–380.
23. Vithlani M, Terunuma M, Moss SJ (2011) The dynamic modulation of GABA(A) receptor trafficking and its role in regulating the plasticity of inhibitory synapses. *Physiol Rev* 91:1009–1022.
24. Knott GW, Quairiaux C, Genoud C, Welker E (2002) Formation of dendritic spines with GABAergic synapses induced by whisker stimulation in adult mice. *Neuron* 34:265–273.
25. Megias M, Emri Z, Freund TF, Gulyas AI (2001) Total number and distribution of inhibitory and excitatory synapses on hippocampal CA1 pyramidal cells. *Neuroscience* 102:527–540.
26. Bartos M, Vida I, Jonas P (2007) Synaptic mechanisms of synchronized gamma oscillations in inhibitory interneuron networks. *Nat Rev Neurosci* 8:45–56.
27. Kullmann DM (2011) Interneuron networks in the hippocampus. *Curr Opin Neurobiol* 21:709–716.
28. Tyagarajan SK, Ghosh H, Yevenes GE, Imanishi SY, Zeilhofer HU, Gerrits B, Fritschy JM (2013) Extracellular signal-regulated kinase and glycogen synthase kinase 3beta regulate gephyrin postsynaptic aggregation and GABAergic synaptic function in a calpain-dependent mechanism. *J Biol Chem* 288:9634–9647.

29. Lisman J, Yasuda R, Raghavachari S (2012) Mechanisms of CaMKII action in long-term potentiation. *Nat Rev Neurosci* 13:169–182.
30. Sohal VS, Zhang F, Yizhar O, Deisseroth K (2009) Parvalbumin neurons and gamma rhythms enhance cortical circuit performance. *Nature* 459:698–702.
31. Donato F, Rompani SB, Caroni P (2013) Parvalbumin-expressing basket-cell network plasticity induced by experience regulates adult learning. *Nature* 504:272–276.
32. Stoppini L, Buchs PA, Muller D (1991) A simple method for organotypic cultures of nervous tissue. *J Neurosci Methods* 37:173–182.
33. Nikonenko I, Boda B, Steen S, Knott G, Welker E, Muller D (2008) PSD-95 promotes synaptogenesis and multiinnervated spine formation through nitric oxide signaling. *J Cell Biol* 183:1115–1127.

Figure legends

Figure 1.Basal turnover of gephyrin-containing inhibitory synapses in rat organotypic hippocampal cultures. *(A)* Low maginification view of a mRFP transfected CA1 pyramidal neuron imaged 8 days after transfection at 19 DIV (scale bar: 10 µm). *(B)* Repetitive imaging at 24h interval of the proximal dendrite of a eGFP-gephyrin transfected neuron. Note the variations in size of gephyrin clusters (green) and the existence of movements (arrow), stable (arrow heads), new (+) and lost (-) clusters (scale bar: 2 µm). *(C)* Quantitative analysis of gephyrin turnover expressed as the fraction of new (filled circles) and lost (open circles) clusters observed over 24h per proximal dendrite (n=11 cells/134 clusters). *(D)* Absence of changes in cluster density under basal conditions. *(E*) Absence of changes in the mean size of gephyrin clusters. *(F)* Confocal projection of an apical proximal dendrite of a pyramidal neuron transfected with eGFP and mCherry-gephyrin (left panel; scale bar: 2 µm). The middle panel shows only the mCherry-gephyrin signal and the right panel illustrates the 3D EM reconstruction of the same dendrite. Red dots represent inhibitory symmetrical synapses and blue dots are the superimposed presynaptic boutons. Note that all small gephyrin clusters correlate with inhibitory synapses, while the large gephyrin clusters correspond to gephyrin accumulations in areas where multiple inhibitory synapses are present. *(G)* Electron microscopic image of the small confocal gephyrin cluster illustrated by the top arrow on the right panel in F. The reconstructed dendrite was identified through eGFP immunolabeling. *(H)* Same but for the large inhibitory synapse corresponding to the large gephyrin cluster illustrated in F (lower arrow; scale bar: 0.2 µm).

Figure 2. Activity-dependent increase in gephyrin cluster dynamics. *(A)* Proximal apical dendrite illustrating the changes in eGFP-gephyrin clusters (+, new clusters; - lost clusters) observed before and 24h after application of 10 μM carbachol for 45 min (scale bar: 2 μm). *(B)* Gephyrin cluster dynamics 24h after theta burst stimulation (TBS). *(C)* Proportion of newly formed gephyrin clusters observed per 24h following Cch application (black squares), TBS (dark circles) and TBS in the presence of 50 μM D-AP5 (grey diamonds). *(D)* Changes in lost gephyrin clusters under the same conditions. *(E)* Changes in size of pre-existing gephyrin clusters. *(F)* Apposition of GAD67 immunostaining with the new gephyrin clusters induced by carbachol treatment (72h after treatment). *(G*) New mCherry-gephyrin clusters (+) observed 24h after TBS and correlated 3D-EM reconstruction of the same dendrite confirming the presence of inhibitory synapses (right image; scale bars: 2 μm). Red dots represent inhibitory symmetrical synapses and blue dots presynaptic boutons.

Figure 3. Increase in gephyrin cluster dynamics by the $GABA_AR$ antagonist gabazine (GBZ). *(A)* Proximal apical dendrite before and 24h after a short GBZ treatment (45 min; scale bar: 2 μm). Note the marked increase in number (+) and size of gephyrin clusters. *(B)* Proportion of new gephyrin clusters observed 24h after a short GBZ treatment (Ctrl, open columns, n=7 cells/ 56 clusters; GBZ, filled columns, n=7 cells/ 49 clusters; *** *p<0.001, one way ANOVA*). (C) Changes in mean size of gephyrin clusters (*** *p<0.001, one way ANOVA*). *(D)* Illustration of mIPSCs recorded in CA1 pyramidal neurons under control conditions (left) and 24h after a short GBZ treatment (right; scale bars: 50pA/50s, top; 100pA/0.5s, bottom). *(E)* Increase in mIPSC frequency (left) and amplitude (right) induced by GBZ (Ctrl, open columns, n=11 cells; GBZ, filled columns, n=11 cells; * *p<0.05, unpaired t-test*).

Figure 4. Optogenetic activation of single pyramidal neurons increases gephyrin cluster dynamics. *(A)* CA1 pyramidal neuron expressing mCherry-gephyrin (red) and ChR2-venus (green, scale bar: 12 μm). *(B)* Representative traces of cell attached recordings obtained at the beginning and end of a short (5 min, 1Hz trains of 5 pulses at 10Hz) optogenetic stimulation (470 nm blue light) of a cell expressing mCherry-gephyrin/ChR2-venus. Each vertical deflection represents an action potential.

(C) Proximal apical dendrite showing new (+) and lost (-) mCherry-gephyrin clusters observed 24h after a 5 min optogenetic stimulation with red light (625 nm). (D) Same as *(C)* but following 5 min stimulation with blue light (470 nm; scale bar: 3 μm). Note the robust increase in new clusters. *(E)* Proportion of new gephyrin clusters observed following stimulation with red and blue light (red light, red columns, n=4 cells; blue light, blue columns, n=5 cells; * *p<0.05, Mann-Whitney U-test*). *(F)* Same as *(E)* but for lost gephyrin clusters. *(G)* Changes in the mean size of gephyrin clusters following red and blue light stimulation (red light, n=4 cells/37 clusters; blue light, n=5 cells/87 clusters, * *p<0.05, one way ANOVA*).

Figure 5. Inhibitory synapse formation through CaMKII-mediated phosphorylation of gephyrin. (A) mCherry-gephyrin clusters (red) observed on a proximal apical dendrite (green) before and 24h after TBS stimulation applied in the presence of KN-93 (10 μM; scale bar: 2 μm). (B) TBS-induced gephyrin cluster dynamics is blocked by KN-93 (10 μM; scale bar: 2 μm). (C) Endogenous gephyrin phosphorylation at S305 is increased by GBZ. (D) Illustration of gephyrin cluster dynamics in neurons transfected with S303D/S305D and S303A/S305A mutants. (E) New gephyrin clusters observed in control conditions and after TBS in neurons transfected with WT, S303A/S305A or S303D/S305D mutants. *(F)* Changes in gephyrin cluster size under the same conditions.

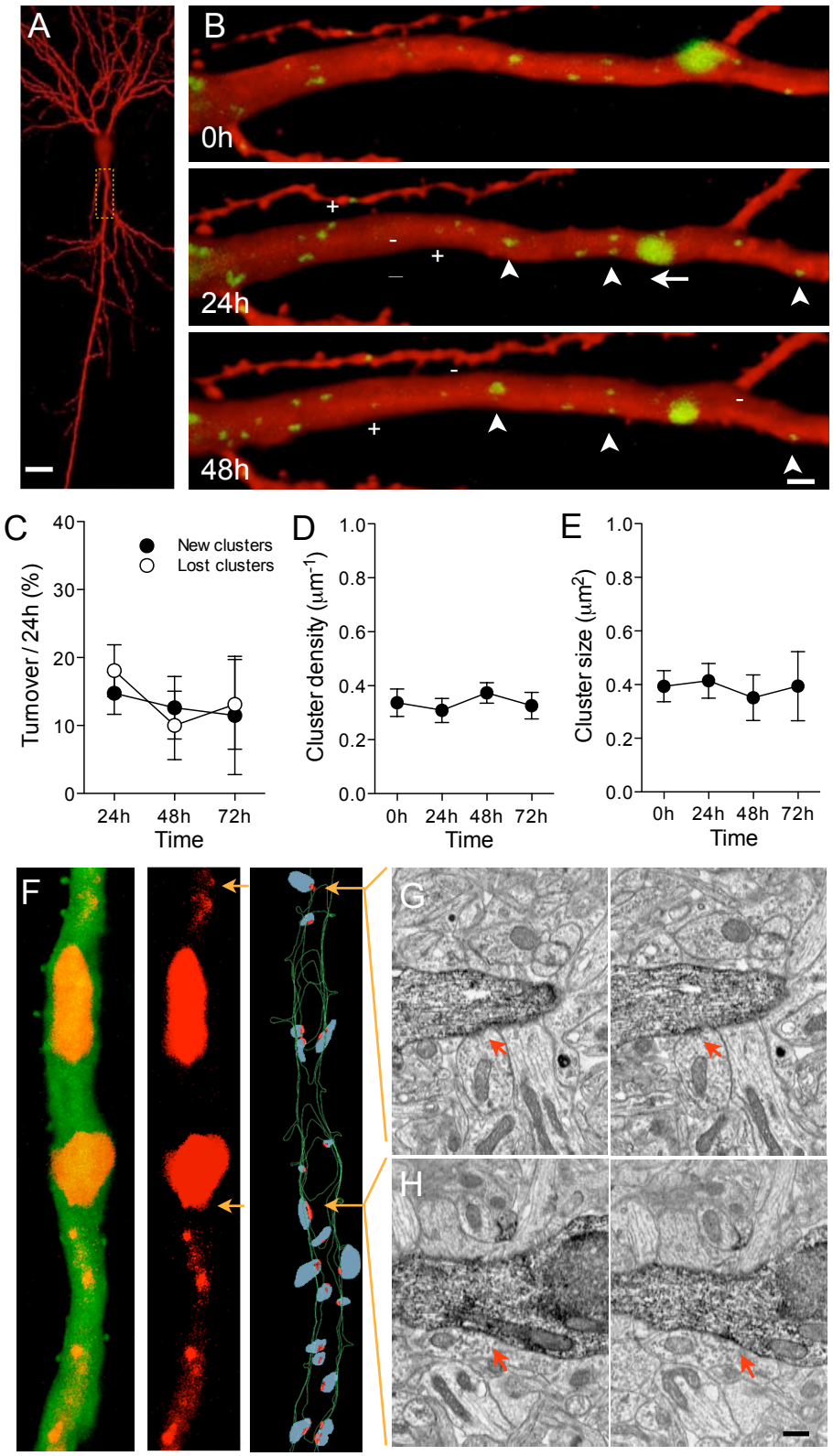

Figure 1
Flores et al.

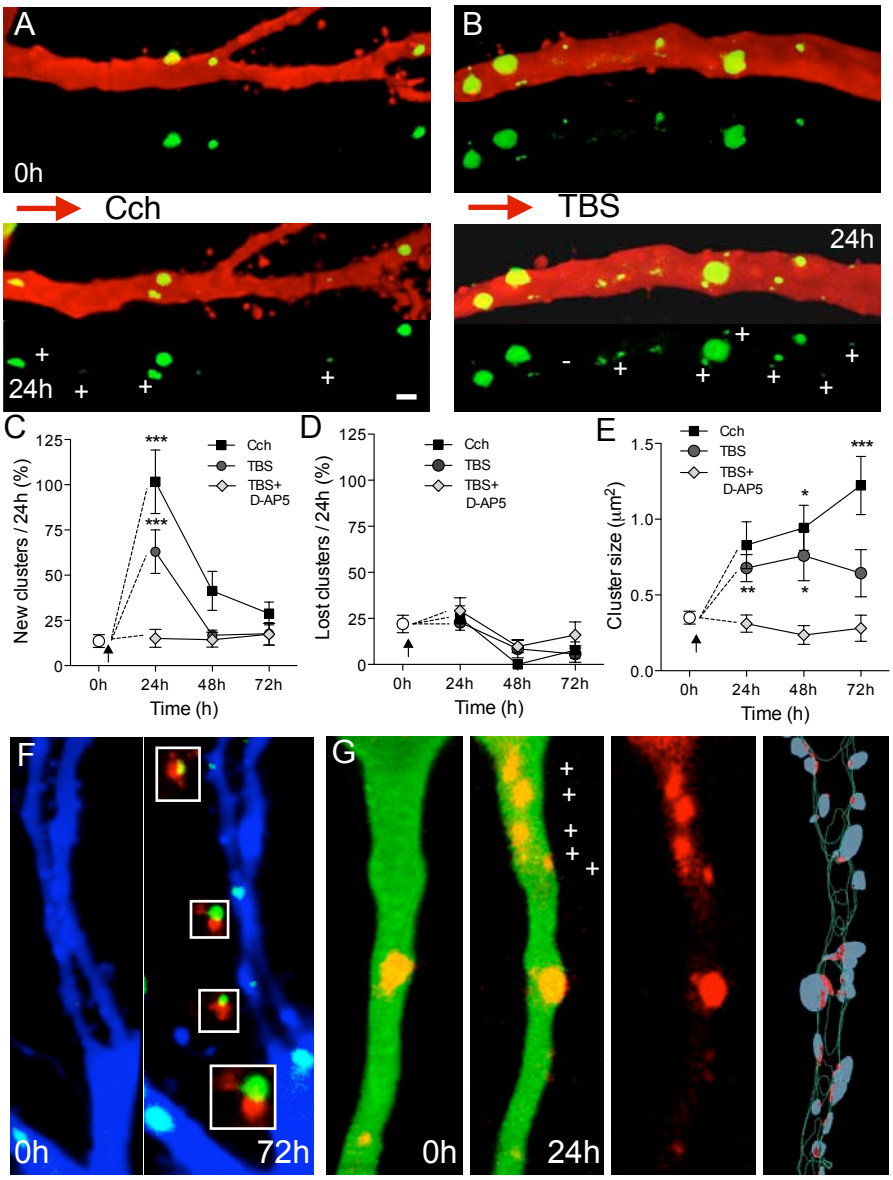

Figure 2
Flores et al.

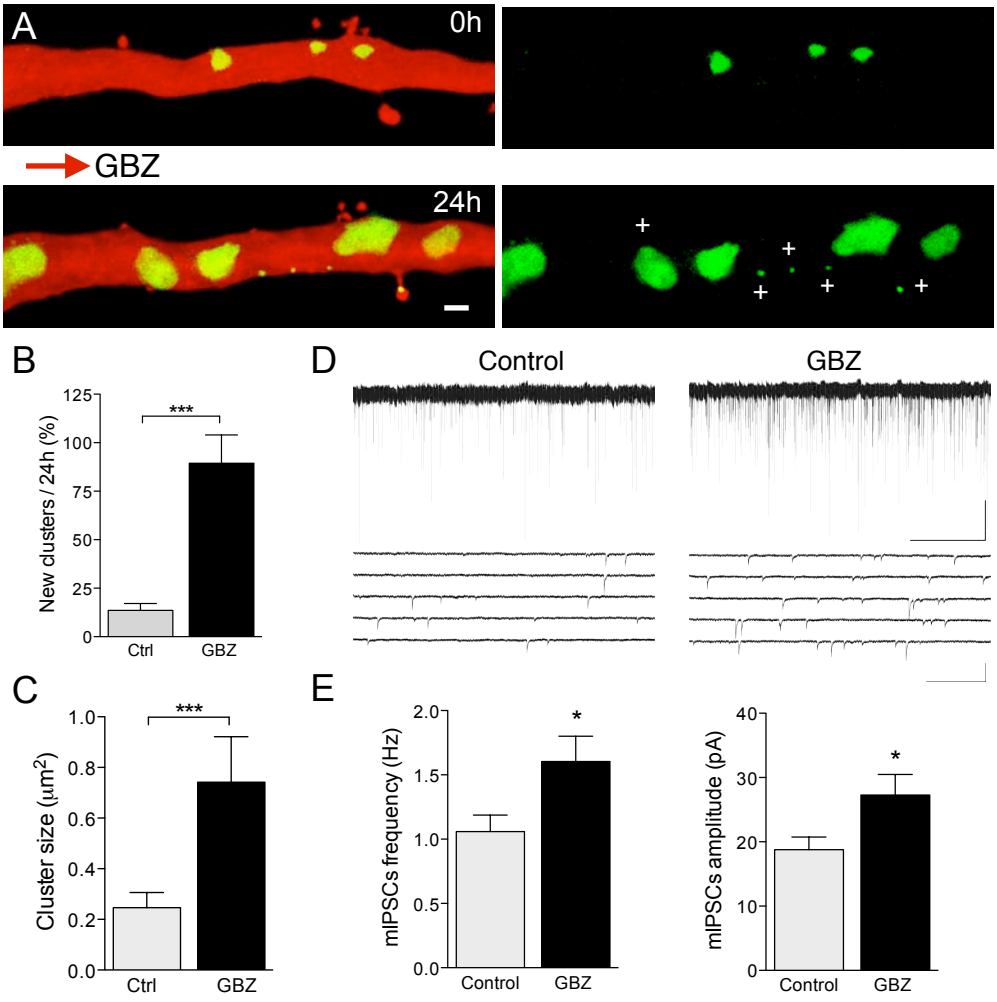

Figure 3
Flores et al.

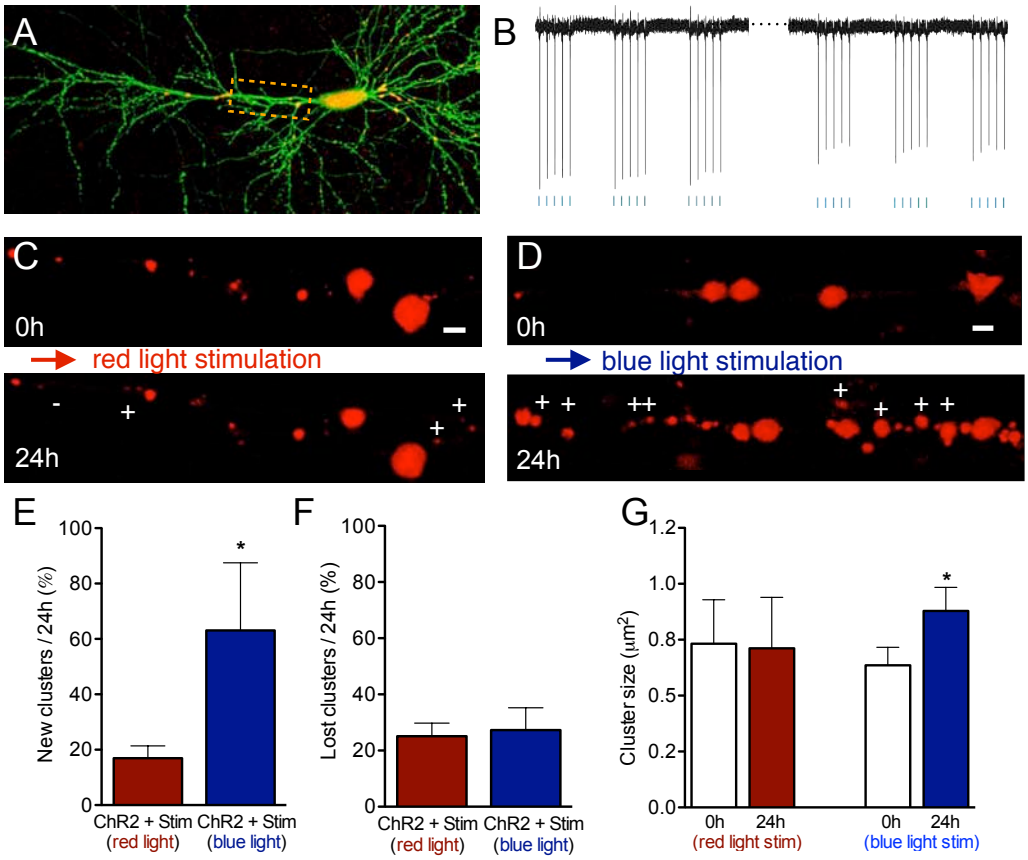

Figure 4
Flores et al.

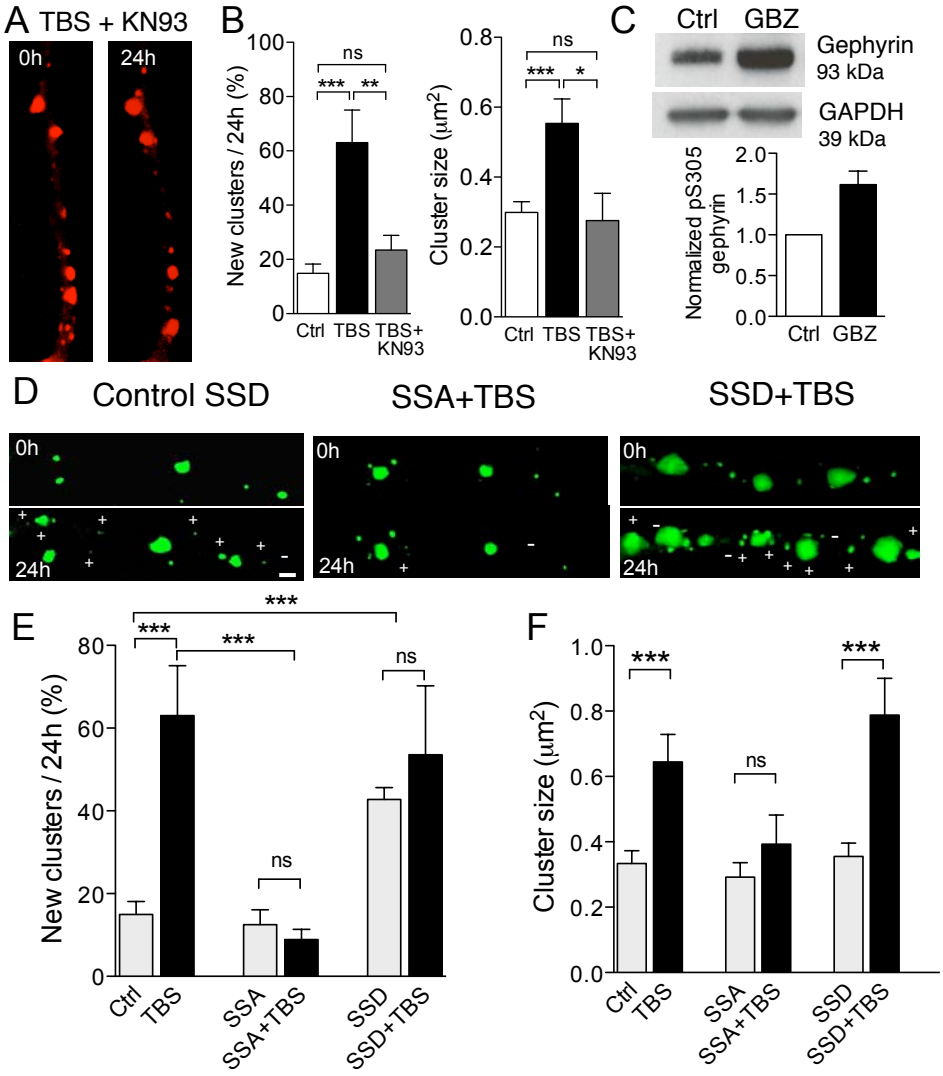

Figure 5
Flores et al.